Supporting Material for

Designing cell targeted therapeutic proteins reveals the interplay between domain connectivity and cell binding

Avi Robinson-Mosher*[1], Jan-Hung Chen*[2], Jeffrey Way[1], and Pamela A. Silver[1,2]
*Co-first author

[1]Wyss Institute for Biologically Inspired Engineering, Harvard University, Boston, MA 02115 USA

[2]Department of Systems Biology, Harvard Medical School, Boston, MA 02115 USA

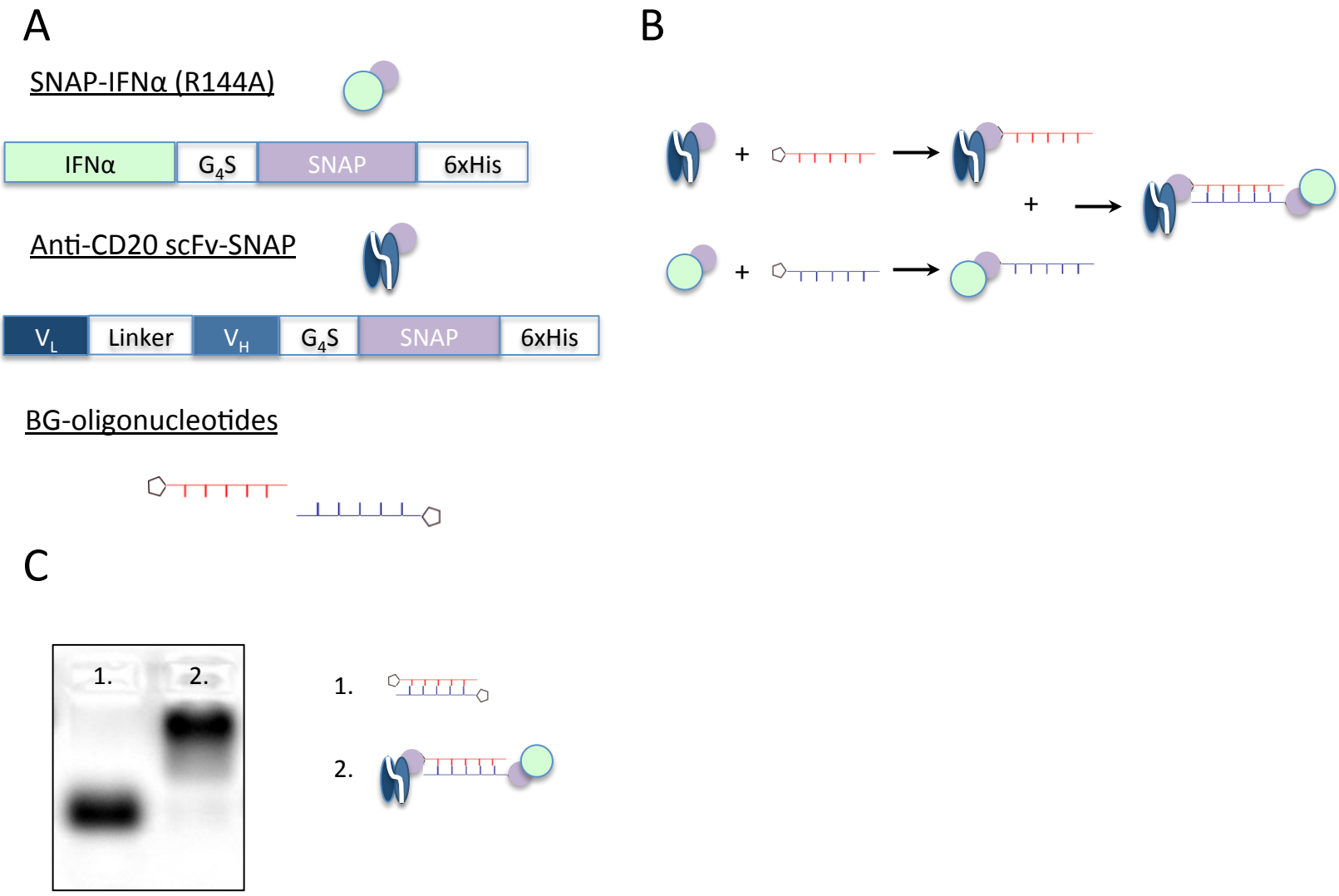

Figure S1. Self-assembled anti-CD20 scFv-DNA-IFNα. (A) The components of the anti-CD20 scFv-DNA-IFNα: SNAP-IFNα, anti-CD20 scFv-SNAP, and BG-modified oligonucleotides. **(B)** To assemble, SNAP-IFNα and anti-CD20 scFv-SNAP were first incubated with the forward and reverse strand of a BG-modified oligonucleotide pair separately. The oligonucleotide-labeled proteins were then mixed 1:1 to allow hybridization to form anti-CD20 scFv-DNA-IFNα. **(C)** The site-specific conjugation of SNAP-tagged protein to BG-oligonucleotide was confirmed in a gel-shift assay. When both anti-CD20 scFv-SNAP and SNAP SNAP-IFNα are conjugated to the DNA linker, there was a band shift (lane 2) compared to DNA linker alone.

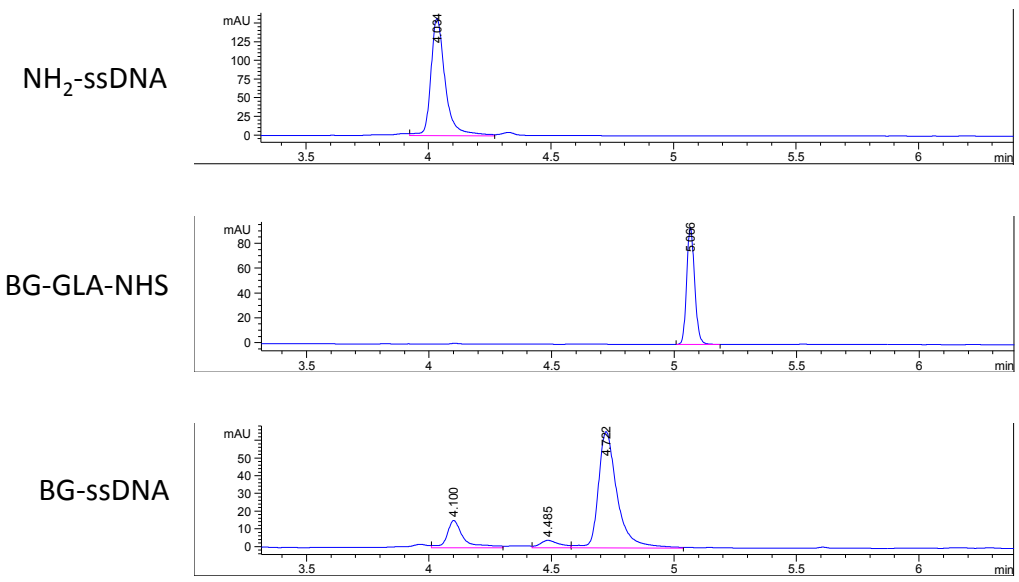

Figure S2. Validation of the BG-DNA conjugation. BG-GLA-NHS was conjugated to amine-modified oligonucleotides. The reaction was purified to remove excess BG-GLA-NHS. The conjugation was verified using HPLC.

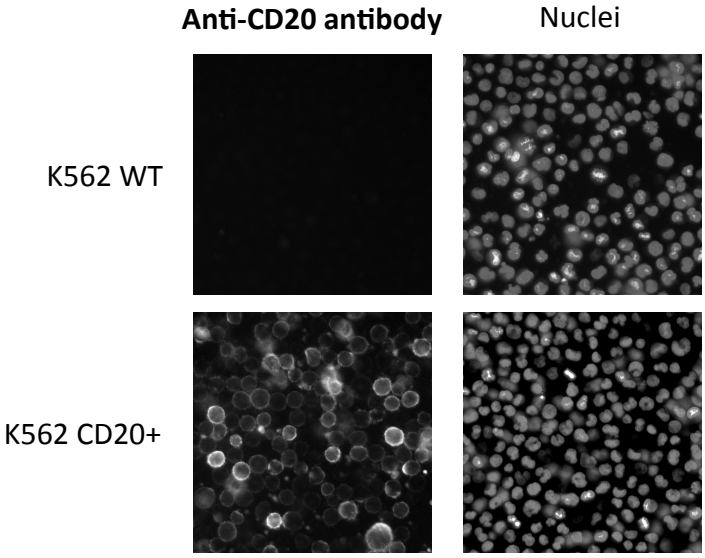

Figure S3. Validating the expression levels of CD20 on the K562 WT and CD20+ cells. We confirmed the membrane expression of CD20 on the K562 WT and CD20+ cell surface by immunofluorescent staining using a commercially available phycoerythrin-conjugated antibody. As expected, K562 WT did not show CD20 immunostaining, whereas the K562 CD20+ cells showed a high level of fluorescent labeling.

Table S1: DNA linker sequences

15 bp	Forward	CAGAACAGCGACAAA
	Reverse	TTTGTCGCTGTTCTG
30 bp	Forward	TTGTCTCGTCTTTGTCTTGTCCTTGTCCTC
	Reverse	GAGGACAAGGACAAGACAAAGACGAGACAA
45 bp	Forward	CCTCTACTCCACTCTACCTCACTCACTACCCTACCCTACCTACCA
	Reverse	TGGTAGGTAGGGTAGGGTAGTGAGTGAGGTAGAGTGGAGTAGAGG

Supplementary Table S2: ODE model

Parameters used in the ODE model

Parameter	Symbol	Value	Source
Cells per well		1.5e5	
Well volume		100μL	
K562 cell surface area		584μm^2	(1)
K562 WT cell IFNAR1 count		1062	Measured by QuantiBrite
K562 WT cell IFNAR2 count		3021	Measured by QuantiBrite
K562 WT cell CD20 count		0	Measured by QuantiBrite
K562 CD20+ cell IFNAR1 count		890	Measured by QuantiBrite
K562 CD20+ cell IFNAR2 count		2725	Measured by QuantiBrite
K562 CD20+ cell CD20 count		250000	Measured by QuantiBrite
IFN WT IFNAR1 on-rate	k_{on}^{R1}	2e5 $M^{-1}s^{-1}$	(2)
IFN WT IFNAR1 off-rate	k_{off}^{R1}	1 s^{-1}	(2)
IFN WT IFNAR2 on-rate	k_{on}^{R2}	3e6 $M^{-1}s^{-1}$	(2)
IFN WT IFNAR2 off-rate	k_{off}^{R2}	1.5e-2 s^{-1}	(2)
IFN WT-GS-SNAP IFNAR1 on-rate	k_{on}^{R1}	2e5 $M^{-1}s^{-1}$	(2)
IFN WT-GS-SNAP IFNAR1 off-rate	k_{off}^{R1}	1 s^{-1}	(2)
IFN WT-GS-SNAP IFNAR2 on-rate	k_{on}^{R2}	2e5 $M^{-1}s^{-1}$	Estimated by fit to experiment
IFN WT-GS-SNAP IFNAR2 off-rate	k_{off}^{R2}	1.5e-2 s^{-1}	(2)
IFN R144A-GS-SNAP IFNAR1 on-rate	k_{on}^{R1}	2e5 $M^{-1}s^{-1}$	(2)
IFN R144A-GS-SNAP IFNAR1 off-rate	k_{off}^{R1}	1 s^{-1}	(2)
IFN R144A-GS-SNAP IFNAR2 on-rate	k_{on}^{R2}	4e4 $M^{-1}s^{-1}$	Estimated by fit to experiment
IFN R144A-GS-SNAP IFNAR2 off-rate	k_{off}^{R2}	5e-2 s^{-1}	(2)
Anti-CD20 scFv CD20 on-rate	k_{on}^{CD}	1e4 $M^{-1}s^{-1}$	Estimated by model fit
Anti-CD20 scFv CD20 off-rate	k_{off}^{CD}	1e-2 s^{-1}	Estimated by model fit
IFNAR1 diffusion coefficient	k_D^{R1}	1e-8 mm^2s^{-1}	(3)
IFNAR2 diffusion coefficient	k_D^{R2}	1e-8 mm^2s^{-1}	(3)
CD20 diffusion coefficient	k_D^{CD}	1e-8 mm^2s^{-1}	(3)
Non-signaling endocytosis rate	k_e^{NS}	9.625e-5 s^{-1}	(4)
Signaling endocytosis rate	k_e^{S}	7.8e-4 s^{-1}	(5)

ODE model transitions

The states tracked in the ODE model are

State	Symbol
Unbound chimeric activator or IFN	F_A
Unbound CD20	F_{CD}
Unbound IFNAR1	F_{R1}
Unbound IFNAR2	F_{R2}
CD20-bound CA	B_C
IFNAR1-bound CA	B_{R1}
IFNAR2-bound CA	B_{R2}
CD20-IFNAR1-bound CA	$B_{CD,R1}$
CD20-IFNAR2-bound CA	$B_{CD,R2}$
IFNAR1-IFNAR2-bound CA	$B_{R1,R2}$
CD20-IFNAR1-IFNAR2-bound CA	$B_{CD,R1,R2}$

All of the reactions that compose the ODE are contained in the table below. All rates of the form "$k_{on}^{CD|R2}$" are calculated according to (3), equation (4-37a), and all rates of the form "$k_{off}^{CD|R2}$" are calculated according to (3), equation (4-38). "$k_{on}^{CD|R2}$" should be read as "the on-rate of binding to CD20 given that the complex is already bound to IFNAR2" and "$k_{off}^{CD|R2}$" should be read as "the rate of complete dissociation from CD20 given that the complex is bound to IFNAR2 and CD20." A state of the form "$B_{CD,R1}$" indicates "chimeric activator bound to both CD20 and IFNAR1."

Reactants	Products	Rate
$\mathbf{F_A, F_{CD}}$	B_{CD}	k_{on}^{CD}
$\mathbf{F_A, F_{R1}}$	B_{R1}	k_{on}^{R1}
$\mathbf{F_A, F_{R2}}$	B_{R2}	k_{on}^{R2}
$\mathbf{F_{CD}, B_{R1}}$	$B_{CD,R1}$	$k_{on}^{CD\|R1}$
$\mathbf{F_{CD}, B_{R2}}$	$B_{CD,R2}$	$k_{on}^{CD\|R2}$
$\mathbf{F_{R1}, B_{R2}}$	$B_{R1,R2}$	$k_{on}^{R1\|R2}$
$\mathbf{B_{R1}, F_{R2}}$	$B_{R1,R2}$	$k_{on}^{R2\|R1}$
$\mathbf{B_{CD}, F_{R1}}$	$B_{CD,R1}$	$k_{on}^{R1\|CD}$
$\mathbf{B_{CD}, F_{R2}}$	$B_{CD,R2}$	$k_{on}^{R2\|CD}$
$\mathbf{F_{CD}, B_{R1,R2}}$	$B_{CD,R1,R2}$	$k_{on}^{CD\|R2}$
$\mathbf{F_{R1}, B_{CD,R2}}$	$B_{CD,R1,R2}$	$k_{on}^{R1\|R2}$
$\mathbf{F_{R2}, B_{CD,R1}}$	$B_{CD,R1,R2}$	$k_{on}^{R2\|R1}$
$\mathbf{B_{CD}}$	F_{CD}, F_A	k_{off}^{CD}
$\mathbf{B_{R1}}$	F_{R1}, F_A	k_{off}^{R1}
$\mathbf{B_{R2}}$	F_{R2}, F_A	k_{off}^{R2}
$\mathbf{B_{CD,R1}}$	F_{CD}, B_{R1}	$k_{off}^{CD\|R1}$
$\mathbf{B_{CD,R1}}$	F_{R1}, B_{CD}	$k_{off}^{R1\|CD}$
$\mathbf{B_{CD,R2}}$	F_{CD}, B_{R2}	$k_{off}^{CD\|R2}$

$\mathbf{B_{CD,R2}}$	F_{R2}, B_{CD}	$k_{off}^{R2\|CD}$
$\mathbf{B_{R1,R2}}$	F_{R1}, B_{R2}	$k_{off}^{R1\|R2}$
$\mathbf{B_{R1,R2}}$	F_{R2}, B_{R1}	$k_{off}^{R2\|R1}$
$\mathbf{B_{CD,R1,R2}}$	F_{CD}, $B_{R1,R2}$	$k_{off}^{CD\|R2}$
$\mathbf{B_{CD,R1,R2}}$	F_{R1}, $B_{CD,R2}$	$k_{off}^{R1\|R2}$
$\mathbf{B_{CD,R1,R2}}$	F_{R2}, $B_{CD,R1}$	$k_{off}^{R2\|R1}$
$\mathbf{B_{CD}}$	None	k_e^{NS}
$\mathbf{B_{R1}}$	None	k_e^{NS}
$\mathbf{B_{R2}}$	None	k_e^{NS}
$\mathbf{B_{CD,R1}}$	None	k_e^{NS}
$\mathbf{B_{CD,R2}}$	None	k_e^{NS}
$\mathbf{B_{R1,R2}}$	None	k_e^{S}
$\mathbf{B_{CD,R1,R2}}$	None	k_e^{S}

State transitions in the form of ordinary differential equations

$$\frac{dF_A}{dt} = B_{CD}k_{off}^{CD} + B_{R1}k_{off}^{R1} + B_{R2}k_{off}^{R2} - F_A F_{CD}k_{on}^{CD} - F_A F_{R1}k_{on}^{R1} - F_A F_{R2}k_{on}^{R2}$$

$$\frac{dF_{CD}}{dt} = B_{CD}k_{off}^{CD} + B_{CD,R1}k_{off}^{CD|R1} + B_{CD,R2}k_{off}^{CD|R2} + B_{CD,R1,R2}k_{off}^{CD|R2} - F_{CD}F_A k_{on}^{CD} - F_{CD}B_{R1}k_{on}^{CD|R1} - F_{CD}B_{R2}k_{on}^{CD|R2} - F_{CD}B_{R1,R2}k_{on}^{CD|R2}$$

$$\frac{dF_{R1}}{dt} = B_{R1}k_{off}^{R1} + B_{CD,R1}k_{off}^{R1|CD} + B_{R1,R2}k_{off}^{R1|R2} + B_{CD,R1,R2}k_{off}^{R1|R2} - F_{R1}F_A k_{on}^{R1} - F_{R1}B_{CD}k_{on}^{R1|CD} - F_{R1}B_{R2}k_{on}^{R1|R2} - F_{R1}B_{CD,R2}k_{on}^{R1|R2}$$

$$\frac{dF_{R2}}{dt} = B_{R2}k_{off}^{R2} + B_{CD,R2}k_{off}^{R2|CD} + B_{R1,R2}k_{off}^{R2|R1} + B_{CD,R1,R2}k_{off}^{R2|R1} - F_{R2}F_A k_{on}^{R2} - F_{R2}B_{CD}k_{on}^{R2|CD} - F_{R2}B_{R1}k_{on}^{R2|R1} - F_{R2}B_{CD,R1}k_{on}^{R2|R1}$$

$$\frac{B_{CD}}{dt} = F_{CD}F_A k_{on}^{CD} + B_{CD,R1}k_{off}^{CD|R1} + B_{CD,R2}k_{off}^{CD|R2} - B_{CD}k_{off}^{CD} - B_{CD}F_{R1}k_{on}^{R1|CD} - B_{CD}F_{R2}k_{on}^{R2|CD} - B_{CD}k_e^{NS}$$

$$\frac{B_{R1}}{dt} = F_{R1}F_A k_{on}^{R1} + B_{CD,R1}k_{off}^{R1|CD} + B_{R1,R2}k_{off}^{R1|R2} - B_{R1}k_{off}^{R1} - B_{R1}F_{CD}k_{on}^{CD|R1} - B_{R1}F_{R2}k_{on}^{R2|R1} - B_{R1}k_e^{NS}$$

$$\frac{B_{R2}}{dt} = F_{R2}F_A k_{on}^{R2} + B_{CD,R2}k_{off}^{R2|CD} + B_{R1,R2}k_{off}^{R2|R1} - B_{R2}k_{off}^{R2} - B_{R2}F_{CD}k_{on}^{CD|R2} - B_{R2}F_{R1}k_{on}^{R1|R2} - B_{R2}k_e^{NS}$$

$$\frac{B_{CD,R1}}{dt} = B_{CD}F_{R1}k_{on}^{R1|CD} + B_{R1}F_{CD}k_{on}^{CD|R1} + B_{CD,R1,R2}k_{off}^{R2|R1} - B_{CD,R1}k_{off}^{CD|R1} - B_{CD,R1}k_{off}^{R1|CD} - B_{CD,R1}F_{R2}k_{on}^{R2|R1} - B_{CD,R1}k_e^{NS}$$

$$\frac{B_{CD,R2}}{dt} = B_{CD}F_{R2}k_{on}^{R2|CD} + B_{R2}F_{CD}k_{on}^{CD|R2} + B_{CD,R1,R2}k_{off}^{R1|R2} - B_{CD,R2}k_{off}^{CD|R2} - B_{CD,R2}k_{off}^{R2|CD} - B_{CD,R2}F_{R1}k_{on}^{R1|R2} - B_{CD,R2}k_e^{NS}$$

$$\frac{B_{R1,R2}}{dt} = B_{R1}F_{R2}k_{on}^{R2|R1} + B_{R2}F_{R1}k_{on}^{R1|R2} + B_{CD,R1,R2}k_{off}^{CD|R2} - B_{R1,R2}k_{off}^{R1|R2} - B_{R1,R2}k_{off}^{R2|R1} - B_{R1,R2}F_{CD}k_{on}^{CD|R2} - B_{R1,R2}k_e^S$$

$$\frac{B_{CD,R1,R2}}{dt} = B_{CD,R1}F_{R2}k_{off}^{R2|R1} + B_{CD,R2}F_{R1}k_{on}^{R1|R2} + B_{R1,R2}F_{CD}k_{on}^{CD|R2} - B_{CD,R1,R2}k_{off}^{CD|R2} - B_{CD,R1,R2}k_{off}^{R1|R2} - B_{CD,R1,R2}k_{off}^{R2|R1} - B_{CD,R1,R2}k_e^S$$

Supporting References

1. Williams, T.E., S. Nagarajan, P. Selvaraj, and C. Zhu. 2000. Concurrent and Independent Binding of Fcγ Receptors IIa and IIIb to Surface-Bound IgG. Biophysical Journal. 79: 1867–1875.

2. Jaks, E., M. Gavutis, G. Uzé, J. Martal, and J. Piehler. 2007. Differential receptor subunit affinities of type I interferons govern differential signal activation. Journal of Molecular Biology. 366: 525–539.

3. Lauffenburger, D.A., and J.J. Linderman. 1996. Receptors: Models for Binding, Trafficking, and Signaling. Oxford University Press on Demand.

4. Beum, P.V., E.M. Peek, M.A. Lindorfer, F.J. Beurskens, P.J. Engelberts, P.W.H.I. Parren, J.G.J. van de Winkel, and R.P. Taylor. 2011. Loss of CD20 and Bound CD20 Antibody from Opsonized B Cells Occurs More Rapidly Because of Trogocytosis Mediated by Fc Receptor-Expressing Effector Cells Than Direct Internalization by the B Cells. The Journal of Immunology. 187: 3438–3447.

5. Dunne, S.L., Z. Bajzer, and S. Vuk-Pavlović. 1990. Kinetics of receptor-mediated uptake and processing of interferon-alpha 2a and tumor necrosis factor-alpha by human tumor cells. Growth Factors. 2: 167–177.